Brief Report

Thermal Confinement Effects in Laser-Polished AM 316L Slots: The Role of Geometry in Internal Surface Response

Aswin Karakadakattil *

Posted Date: 2 March 2026

doi: 10.20944/preprints202603.0074.v1

Keywords: laser polishing; additive manufacturing (AM) 316L; thermal confinement; depth-dependent microhardness; slot and channel geometries; microstructure–property relationship; biomedical and aerospace components

 doi:10.20944/preprints202603.0074.v1

Brief Report

Thermal Confinement Effects in Laser-Polished AM 316L Slots: The Role of Geometry in Internal Surface Response

Aswin Karkadakattil

Independent Researcher, India; ashwinharik20000@gmail.com

Abstract

Laser polishing (LP) is widely used to improve the surface quality of additively manufactured (AM) metals; however, its behaviour within deep or narrow internal geometries remains insufficiently understood. Many high-performance AM components including biomedical implants, turbine cooling channels, and metal microfluidic devices contain confined internal features where heat-transfer conditions differ substantially from those at open surfaces. In this study, LPBF-fabricated 316L stainless steel specimens containing ~10 mm deep slots with widths ranging from 1 to 5 mm were laser polished to examine how internal geometry influences microstructural evolution and mechanical response. A clear depth-dependent microhardness gradient was observed along the slot wall, with hardness decreasing from approximately 270 HV in the lower region to about 210 HV toward the slot opening. The gradient was more pronounced in narrower slots. Microstructural characterization revealed finer grains near the slot base and progressively coarser grains toward the upper regions. These variations are consistent with differences in conductive coupling to the surrounding bulk substrate along the slot depth, which influence local cooling conditions during solidification. The results provide quantitative evidence that internal geometric boundary conditions can affect microstructure and hardness development during laser polishing, even when nominal processing parameters are held constant. This work highlights the importance of considering feature geometry in the post-processing of AM components containing confined internal structures and offers guidance for achieving more predictable local mechanical performance.

Keywords: laser polishing; additive manufacturing (AM) 316L; thermal confinement; depth-dependent microhardness; slot and channel geometries; microstructure–property relationship; biomedical and aerospace components

1. Introduction

1.1. Background

Metal additive manufacturing (AM), particularly laser powder bed fusion (LPBF) of 316L stainless steel, enables the fabrication of components with highly complex geometries, including internal channels, enclosed cavities, and architected internal features that are difficult or impossible to produce using conventional subtractive routes [1–3]. These capabilities have accelerated adoption in demanding applications such as biomedical implants, aerospace cooling passages, compact heat exchangers, and metal-based microfluidic systems [4–7]. Despite these advantages, as-built LPBF components frequently exhibit surface-related limitations, including partially fused powder particles, high surface roughness, and microstructural heterogeneity. These features can adversely affect fatigue life, corrosion resistance, flow behaviour, and overall mechanical performance [8–10]. Consequently, post-processing is often required to achieve functional reliability. Laser polishing (LP) has emerged as a promising non-contact post-processing technique for improving surface finish in AM metals. By remelting a thin surface layer, LP promotes material redistribution driven by surface

 doi:10.20944/preprints202603.0074.v1

tension, reducing asperities while simultaneously modifying near-surface microstructure [11–14]. Compared with mechanical polishing, LP is particularly attractive for complex AM geometries because it does not require direct tool access. For open and planar surfaces, the thermal behaviour during laser polishing is relatively well understood. Heat dissipation into the surrounding bulk material and environment is largely unconstrained, and predictable improvements in roughness and microstructure have been reported [15,16]. However, many practical AM components contain internal or partially enclosed features where boundary conditions differ substantially from open-surface configurations. Recent studies have shown that curvature, confinement, and geometric complexity influence melt-pool behaviour, heat-flow pathways, and solidification kinetics during laser processing [17–19]. In confined geometries such as deep slots or narrow channels, conductive and convective heat-transfer pathways are altered relative to open surfaces. As a result, local thermal gradients and cooling rates may vary along the depth of the feature. Fundamental investigations of laser–material interaction further demonstrate that conduction pathways, boundary conditions, and melt-pool stability strongly influence solidification behaviour and resulting microstructure [22–25]. Since grain refinement and hardness are highly sensitive to cooling rate, even modest changes in thermal extraction conditions can produce measurable variations in grain size and mechanical response [26,27]. While microhardness gradients have been reported within melt pools and deposited layers in AM processes [28,29], comparatively little attention has been given to depth-dependent microstructural evolution within laser-polished confined internal features. Quantitative grain-size characterization tools such as ImageJ analysis [30] combined with ASTM E112 protocols [31] provide robust methods for evaluating such variations, yet their application to laser-polished internal AM geometries remains limited. From a physical metallurgy perspective, understanding how geometric boundary conditions influence heat extraction and solidification during LP is essential for establishing reliable process–microstructure–property relationships in confined features.

1.2. Gap in Knowledge

Most laser polishing studies implicitly consider open-surface conditions, where heat can dissipate freely into the bulk material and surrounding environment [11–16]. While appropriate for external surfaces, this assumption does not fully represent the thermal boundary conditions present in confined internal geometries. In deep or narrow slots, heat extraction pathways may differ along the feature depth due to variations in conductive coupling with the bulk substrate and exposure to the surrounding environment. Although theoretical and numerical studies suggest that geometric confinement can modify melt-pool dynamics and cooling behaviour [22–25,32,46], systematic experimental quantification of depth-dependent microhardness and grain-size evolution in laser-polished internal AM slots remains limited. This knowledge gap is particularly significant because internal surfaces frequently govern the long-term reliability of aerospace cooling channels, microfluidic devices, and biomedical implants, where local microstructural stability and mechanical integrity are critical [33–35].

1.3. Purpose of This Work

The objective of this study is to investigate how confined slot geometry influences microhardness and microstructural evolution during laser polishing of LPBF 316L stainless steel. By analysing lower, middle, and upper regions of ~10 mm deep slots with widths ranging from 1 to 5 mm, this work quantifies depth-dependent variations in hardness and grain size under controlled processing conditions. The study focuses on experimentally characterizing the relationship between geometric boundary conditions, cooling-rate variation, grain refinement, and mechanical response within confined internal features.

1.4. Contribution Summary

This study provides the following contributions:

 doi:10.20944/preprints202603.0074.v1

- It systematically quantifies depth-dependent microhardness variation within laser-polished internal AM slots.
- It demonstrates that slot geometry influences hardness gradients under otherwise constant processing parameters.
- It establishes a microstructure–property correlation between grain size evolution and hardness using ImageJ-based analysis and ASTM E112 grain-size measurements.
- It provides application-relevant insights into how internal feature geometry can influence local mechanical response during laser post-processing of AM components.

2. Results

2.1. Geometry-Dependent Thermal Behaviour

Laser–material interaction within the narrow internal slots altered the local heat-transfer conditions during polishing relative to open-surface configurations. The slot walls were spaced 1–5 mm apart and extended approximately 10 mm in depth, as shown in Figure 1(B). Polishing was conducted using a continuous-wave fibre laser ($\lambda \approx 1060$–1080 nm) at powers of 80–120 W and scan speeds of 450–750 mm/s, with nitrogen shielding gas supplied to stabilize the melt pool and limit oxidation. In these confined geometries, the thermal boundary conditions vary along the slot height. The lower region of the slot is in direct conductive contact with the surrounding bulk substrate, providing an efficient pathway for heat extraction into the underlying material. In contrast, regions closer to the slot opening experience comparatively reduced conductive coupling and partial exposure to the surrounding environment, altering local heat dissipation characteristics. As a result, depth-dependent differences in cooling behaviour are established during laser polishing. The lower region, which is more strongly coupled to the bulk material, is expected to experience enhanced conductive heat extraction and consequently higher effective cooling rates following laser passage. Toward the upper region, where conductive pathways differ and environmental exposure becomes more significant, cooling rates are comparatively reduced. This geometry-dependent variation in thermal extraction becomes more pronounced as slot width decreases, since narrower geometries modify lateral heat-flow pathways and constrain melt-pool dimensions. The observed microstructural and hardness gradients along the slot wall are consistent with these depth-dependent thermal conditions.

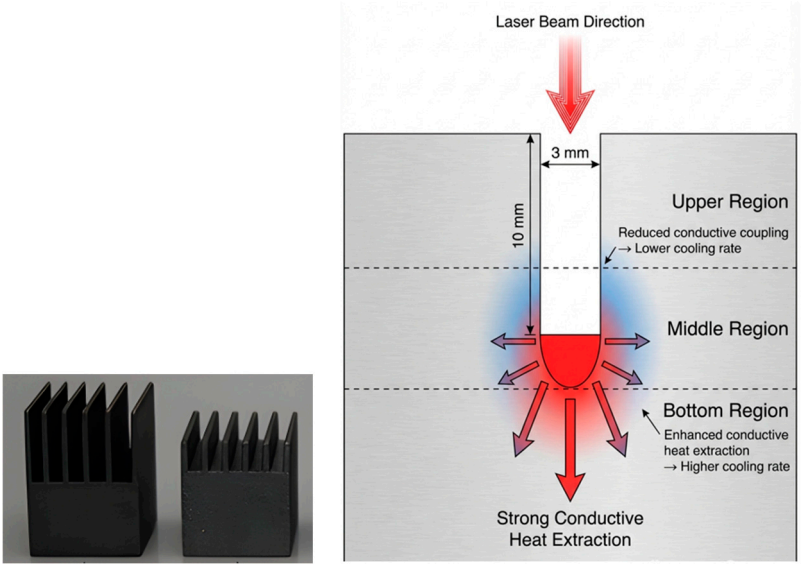

Figure 1. (A) Photograph of the additively manufactured LPBF 316L stainless steel specimen containing internal slots used for laser polishing experiments. (B) Schematic illustration of laser polishing within a narrow internal

 doi:10.20944/preprints202603.0074.v1

slot (1–5 mm width, ~10 mm depth), showing geometry-dependent heat extraction during processing. The lower region of the slot is in direct conductive contact with the surrounding bulk substrate, promoting enhanced heat extraction and relatively higher cooling rates following laser passage. Toward the slot opening, conductive coupling differs due to geometric boundary conditions and environmental exposure, resulting in comparatively lower cooling rates. These depth-dependent variations in thermal behaviour influence solidification conditions, grain evolution, and the resulting microhardness Gradient observed along the polished slot wall.

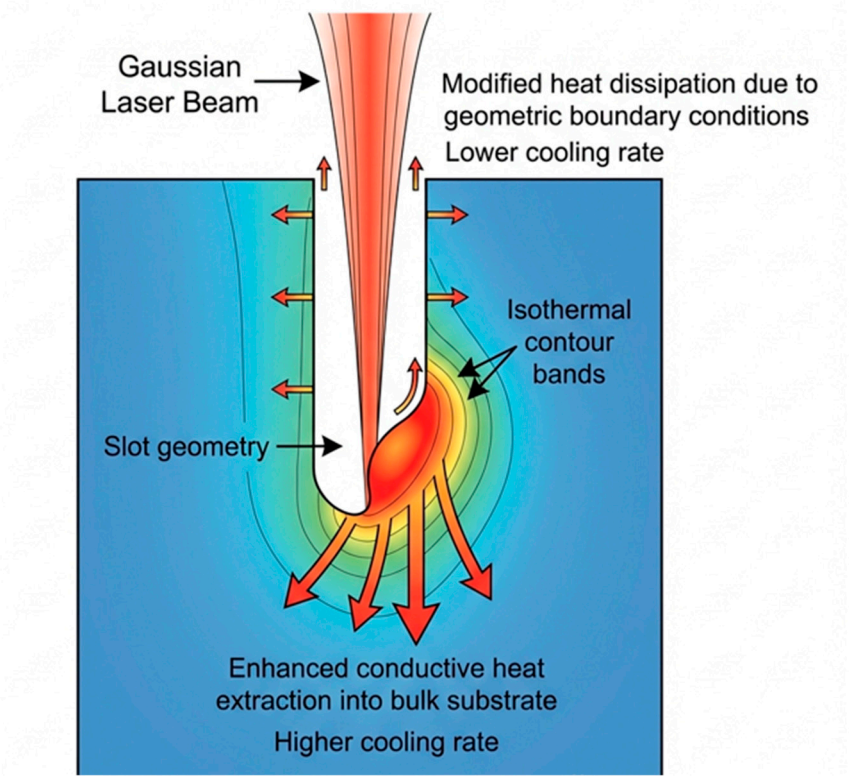

Figure 2. Schematic representation of heat transfer during laser polishing inside a narrow internal slot. The Gaussian laser beam generates a localized heat source along the slot wall. Due to geometric boundary conditions, heat extraction varies along the slot depth. The lower region is in strong conductive contact with the surrounding bulk substrate, promoting enhanced heat extraction and relatively higher cooling rates. Toward the slot opening, heat dissipation conditions differ due to altered conductive pathways and environmental exposure, resulting in comparatively lower cooling rates. The isothermal contour bands illustrate the depth-dependent thermal field established during processing.

2.2. Depth-Resolved Microhardness Gradient

To quantify the mechanical response associated with geometry-dependent heat extraction, Vickers micro-indentation hardness ($HV_{0.5}$) measurements were performed at three defined depths along the slot wall: the lower region (~1 mm from the polished melt zone), the middle region (~5 mm), and the upper region (~10 mm). Five micro-indents were obtained at each depth, and the mean values are presented in Figure 3. Across all slot widths (1–4 mm), a consistent decrease in hardness with increasing height along the slot wall was observed. For example, in the 3 mm slot, hardness decreased from 271 HV in the lower region to 249 HV in the upper region. Similar depth-dependent trends were evident for the other geometries. This systematic gradient is consistent with depth-dependent variations in cooling behaviour during laser polishing. The lower region, which is more strongly coupled to the bulk substrate, is expected to experience enhanced conductive heat extraction and comparatively higher cooling rates following laser passage. In contrast, regions nearer the slot opening exhibit comparatively lower cooling rates due to altered thermal boundary conditions. The observed hardness variation therefore correlates with the corresponding grain-size differences

 doi:10.20944/preprints202603.0074.v1

discussed in Section 2.3. Overall, the results demonstrate a clear relationship between slot geometry, depth position, and microhardness evolution under constant processing parameters.

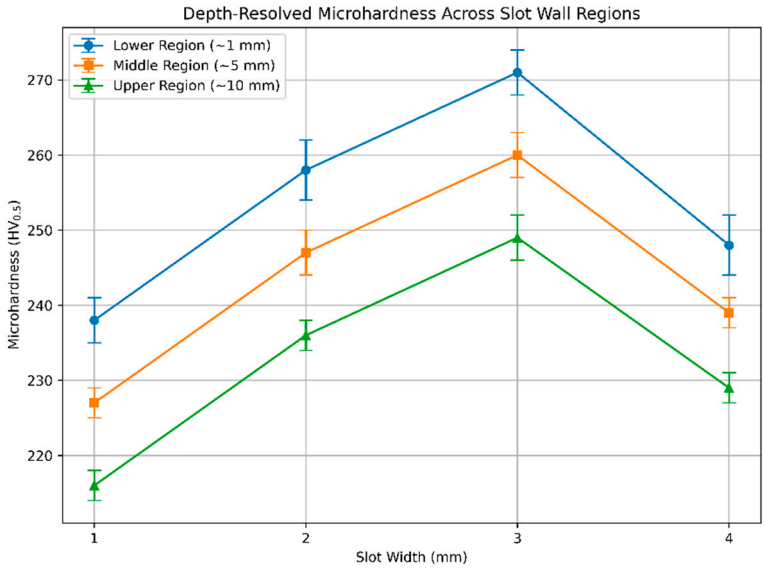

Figure 3. Depth-resolved microhardness of the laser-polished slot wall measured at the lower (~1 mm), middle (~5 mm), and upper (~10 mm) regions for slot widths of 1–4 mm. Error bars represent mean ± standard deviation (n = 5). A consistent decrease in hardness with increasing height along the slot wall is observed across all geometries. The lower region exhibits the highest hardness, followed by the middle and upper regions. This systematic gradient is consistent with depth-dependent variations in cooling behaviour during laser polishing, where enhanced conductive heat extraction near the lower region promotes comparatively higher cooling rates and finer grain structures, while regions closer to the slot opening experience comparatively lower cooling rates and reduced hardness.

Table 1. Depth-resolved microhardness values (mean $HV_{0.5}$) for slot widths of 1–4 mm.

Slot Width (mm)	Lower HV	Middle HV	Upper HV
1	238	227	216
2	258	247	236
3	271	260	249
4	248	239	229

The lower region consistently exhibited the highest hardness, followed by the middle and upper regions. For example, in the 3 mm slot, hardness decreased from 271 HV in the lower region to 249 HV in the upper region (see Figure 3). This depth-dependent trend was observed across all slot widths. The observed gradient is consistent with geometry-dependent variations in heat extraction during laser polishing. The lower region of the slot is in strong conductive contact with the surrounding bulk substrate, promoting enhanced heat extraction and comparatively higher cooling rates following laser passage. In contrast, regions closer to the slot opening experience comparatively reduced conductive coupling and modified thermal boundary conditions, leading to relatively lower cooling rates. These cooling-rate variations correlate with the grain-size differences discussed in Section 2.3. According to Hall–Petch behaviour, finer grains contribute to higher hardness, while coarser grains correspond to reduced hardness. The magnitude of the hardness difference between

 doi:10.20944/preprints202603.0074.v1

the lower and upper regions (ΔHV = HV_lower − HV_upper) varies with slot width. Slots in the 1–3 mm range exhibited larger ΔHV values compared to the 4 mm slot, suggesting that intermediate geometries produce more pronounced depth-dependent thermal gradients under the present processing conditions.

2.3. Microstructure Evolution

Optical micrographs of the laser-polished slot walls reveal clear depth-dependent variations in grain morphology. The specimens were metallographically prepared using standard grinding and polishing procedures and etched with aqua regia to delineate grain boundaries suitable for quantitative analysis. Grain-size measurements were performed using ImageJ, employing thresholding and watershed segmentation for boundary detection and area-based grain quantification. The results were cross-validated using a linear-intercept method, and both approaches showed good agreement. As illustrated in Figure 4, the lower region of the slot exhibits finer equiaxed grains compared to the middle and upper regions. In contrast, the upper region shows comparatively coarser grains. These microstructural differences are consistent with the depth-dependent cooling behaviour described in Section 2.1. The lower region, which is more strongly coupled to the bulk substrate, is expected to experience enhanced conductive heat extraction and relatively higher cooling rates following laser passage. Regions nearer the slot opening exhibit comparatively lower cooling rates due to modified thermal boundary conditions. The observed grain refinement toward the lower region correlates with the higher hardness values reported in Section 2.2. According to the Hall–Petch relationship, reduced grain size contributes to increased hardness, whereas coarser grains correspond to lower hardness. The combined microstructural and hardness data therefore indicate a systematic depth-dependent microstructure–property relationship within the laser-polished slot geometry.

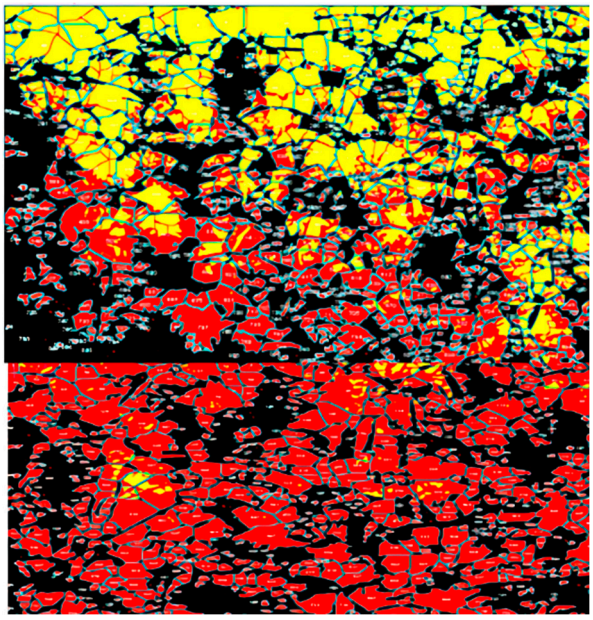

a

 doi:10.20944/preprints202603.0074.v1

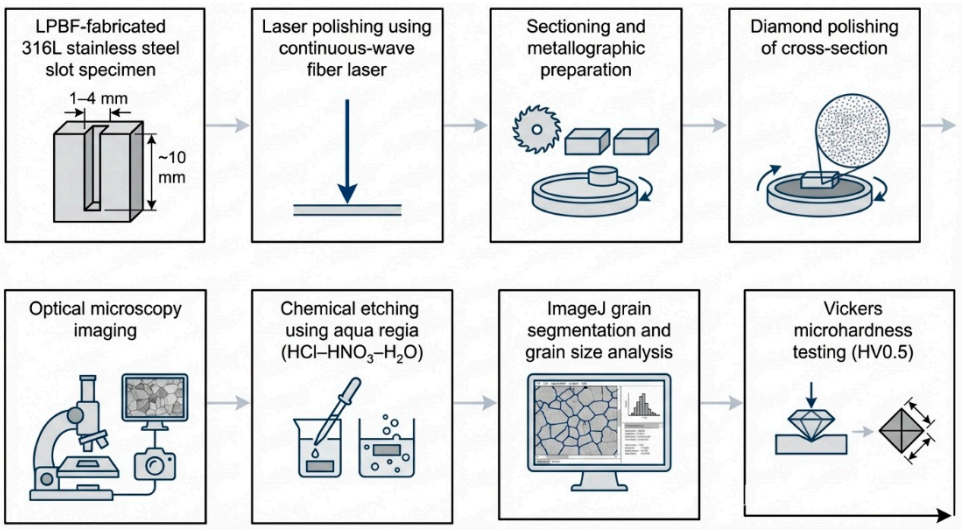

b

Figure 4. (a) ImageJ-assisted grain segmentation of optical micrographs obtained from the laser-polished 316L slot wall after metallographic preparation and etching with aqua regia (HCl–HNO_3–H_2O mixture). The upper portion of the image corresponds to the lower region of the slot (~1 mm from the polished surface), while the lower portion corresponds to the upper region (~10 mm). Grain boundaries were detected using thresholding and watershed segmentation in ImageJ, and grain sizes were quantified using area-based measurements and cross-validated using the linear-intercept method. Finer grains are observed in the lower region, while comparatively coarser grains appear toward the slot opening. These grain-size differences correlate with the depth-dependent hardness measurements shown in Figure 5 and are consistent with Hall–Petch behaviour. (b) Schematic representation of the experimental workflow, including LPBF fabrication of the 316L slot specimen, laser polishing using a continuous-wave fibre laser, sectioning and metallographic preparation, diamond polishing of the cross-section, chemical etching with aqua regia, optical microscopy imaging, ImageJ-based grain segmentation, and Vickers microhardness testing ($HV_{0.5}$).

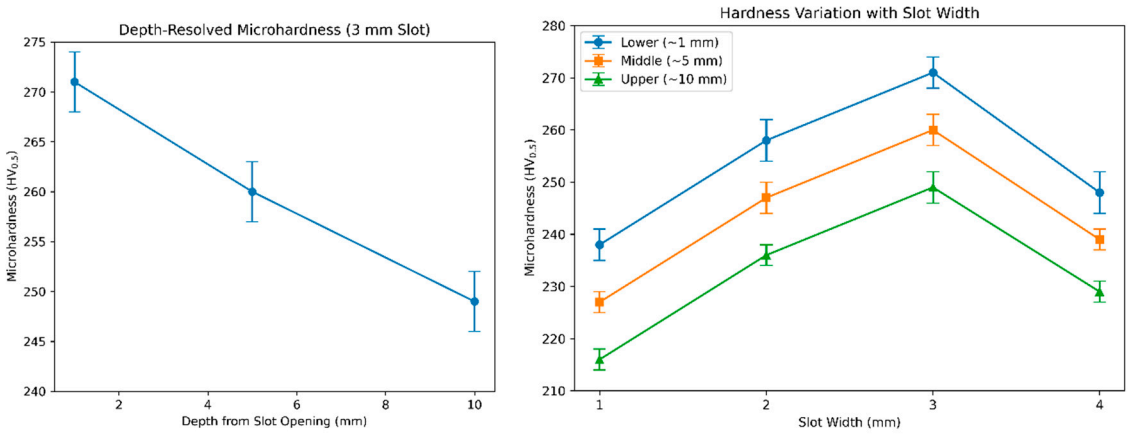

a b

Figure 5. (a) Depth-resolved Vickers microhardness ($HV_{0.5}$) measured at approximately 1 mm (lower region), 5 mm (middle region), and 10 mm (upper region) below the slot opening. Error bars represent mean ± standard deviation from multiple indentations (n = 5). A systematic decrease in hardness from the lower to the upper region is observed, consistent with depth-dependent variations in cooling behaviour during laser polishing. (b) Variation of microhardness with slot width (1–4 mm) for the lower, middle, and upper regions. Hardness values vary with slot geometry at all depths, indicating that geometric boundary conditions influence the local

 doi:10.20944/preprints202603.0074.v1

solidification response. The depth-dependent ordering (lower > middle > upper) is maintained across all slot widths.

3. Discussion

3.1. Mechanistic Interpretation

The results indicate that the mechanical response of laser-polished internal slots is strongly influenced by geometry-dependent thermal boundary conditions. During laser polishing, localized melting occurs along the slot wall, and subsequent solidification is governed by the available heat extraction pathways. In the slot geometries examined (1–4 mm width, ~10 mm depth), the lower region of the slot is in direct conductive contact with the surrounding bulk substrate. This configuration promotes enhanced heat extraction into the underlying material, leading to comparatively higher cooling rates following laser passage. In contrast, regions closer to the slot opening experience altered thermal boundary conditions due to geometric exposure and modified conductive pathways, resulting in comparatively lower cooling rates. The depth-resolved hardness trends shown in Figure 1 reflect this behaviour, with hardness decreasing systematically from the lower to the upper region. The microstructural observations in Section 2.3 demonstrate finer grains in the lower region and coarser grains toward the top, consistent with cooling-rate-dependent solidification. According to the Hall–Petch relationship, reduced grain size contributes to increased hardness, providing a mechanistic link between thermal extraction behaviour and mechanical response. The variation of hardness with slot width (Figure 2) further indicates that geometry influences the magnitude of the depth-dependent gradient. Slots in the 1–3 mm range exhibit similar hardness differentials between lower and upper regions, while the 4 mm slot shows a reduced gradient. This non-monotonic behaviour suggests that an intermediate slot width may produce a balance between conductive heat extraction into the substrate and lateral heat dissipation along the slot walls under the present processing conditions. The hardness difference between lower and upper regions (ΔHV, Figure 3) therefore reflects geometry-dependent variations in cooling behaviour rather than changes in laser power or scan speed, which were held constant. While direct temperature measurements were not performed, the combined hardness and grain-size data consistently indicate a depth-dependent microstructure–property relationship governed by geometric boundary conditions during laser polishing.

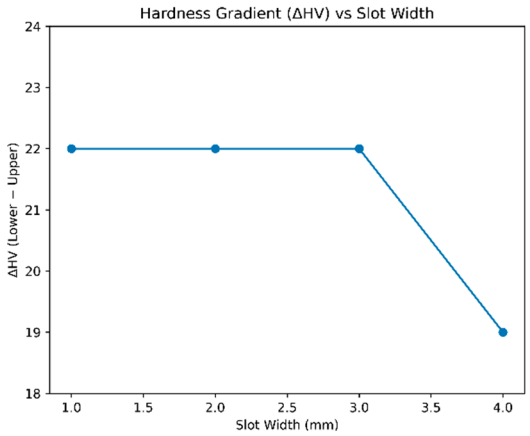

Figure 6. Hardness difference (ΔHV = HV_lower − HV_upper) plotted as a function of slot width. The hardness differential remains approximately constant for slot widths of 1–3 mm and decreases for the 4 mm slot. This indicates that the magnitude of the depth-dependent hardness contrast varies with slot geometry under the present processing conditions. The plot illustrates the geometry-dependent nature of the microhardness gradient without implying a linear or monotonic relationship.

 doi:10.20944/preprints202603.0074.v1

3.2. Engineering Relevance

The findings of this study are relevant to technologies that incorporate internal channels, narrow features, and complex three-dimensional geometries. In biomedical engineering, laser-polished internal surfaces in implants and surgical instruments require controlled surface integrity and consistent mechanical response. Understanding how geometric boundary conditions influence cooling behaviour during laser polishing contributes to improved control of internal surface properties. In microscale heat exchangers and metal microfluidic systems, internal wall characteristics influence flow resistance, heat transfer efficiency, and structural durability. The present results indicate that internal geometry can affect local microstructure and hardness following laser polishing, which may be considered during design and post-processing optimization. Similarly, aerospace cooling passages and additively manufactured turbine components depend on reliable internal surface properties under demanding thermomechanical conditions. The observed depth-dependent hardness variations suggest that geometry may influence local solidification behaviour during polishing. Recognizing such geometry–process interactions can support more informed design strategies aimed at achieving uniform or application-specific internal properties. Overall, these insights align with the broader objective of integrating materials behaviour, advanced manufacturing, and functional performance in complex additively manufactured systems.

3.3. Innovation and Impact

This work demonstrates that internal geometry can influence the mechanical response of laser-polished features even when nominal processing parameters are held constant. The measured depth-dependent gradients in hardness and grain structure indicate a geometry–process interaction that has received limited systematic experimental attention in confined additive-manufactured features. The results suggest that geometric boundary conditions can influence cooling behaviour during solidification and thereby affect the resulting microstructure–property relationship. While direct thermal measurements were not performed, the consistent correlation between grain size and hardness supports a Hall–Petch-type interpretation of the observed gradients. From a design perspective, these findings highlight the importance of considering internal geometry when optimizing laser polishing strategies for complex components. Adjustments in feature dimensions or polishing conditions may be used to reduce property variations or tailor local mechanical response where required. Future work should incorporate transient thermal simulations and direct temperature measurements to quantify heat-transfer behaviour within confined geometries. Extending the study to curved, branched, or interconnected channels would further clarify how geometric complexity influences polishing outcomes. Additional mechanical evaluations, including fatigue or corrosion performance, would strengthen the link between microstructure modification and service behaviour.

4. Limitations and Future Directions

Several limitations define the scope of the present study and identify opportunities for further investigation.

First, the experiments were conducted on straight rectangular slots (1–4 mm width, ~10 mm depth). Although this geometry captures essential aspects of confined polishing conditions, real components often contain curved, tapered, or branched internal channels. Evaluating more complex geometries would provide broader insight into geometry-dependent behaviour.

Second, the mechanical response was assessed primarily through microhardness and grain-size measurements. While these metrics are well established indicators of near-surface strengthening, additional characterization—such as fatigue resistance, corrosion behaviour, or wear performance—would enhance application-level relevance.

Third, direct thermal measurements and numerical modelling were not performed. Incorporating validated transient heat-transfer simulations would provide quantitative prediction of

 doi:10.20944/preprints202603.0074.v1

cooling rates and temperature distributions within confined geometries, strengthening the mechanistic understanding.

Finally, the study employed a continuous-wave fibre laser within a limited parameter range. Exploring alternative laser modes, scanning strategies, or energy densities may reveal additional opportunities for controlling microstructure evolution inside internal features.

These limitations do not diminish the principal observation that internal geometry can influence microstructure and hardness during laser polishing. Rather, they establish a foundation for future studies aimed at integrating process modelling, experimental validation, and application-driven design.

5. Conclusion

This study investigates the influence of internal slot geometry on the mechanical and microstructural response of laser-polished additively manufactured 316L stainless steel. For slot widths of 1–4 mm and a depth of approximately 10 mm, a consistent depth-dependent microhardness gradient was observed, with the lower regions exhibiting higher hardness than the middle and upper regions. The measured hardness variations correlate with corresponding differences in grain morphology, where finer grains were observed in the lower regions and comparatively coarser grains toward the slot opening. These observations are consistent with depth-dependent variations in cooling behaviour during laser polishing, which are influenced by geometric boundary conditions and conductive heat extraction into the surrounding material. The relationship between grain refinement and increased hardness follows established Hall–Petch principles. The results indicate that internal geometry can influence local microstructure and hardness even when nominal laser parameters are maintained constant. This geometry–process interaction highlights the importance of considering feature dimensions and boundary conditions during post-processing of additively manufactured components. From an application perspective, the findings are relevant to components containing internal channels or confined features, such as biomedical devices, aerospace cooling passages, and compact thermal systems. Recognizing geometry-dependent variations in polishing response may support improved design and process optimization for achieving consistent internal material properties. Overall, this work demonstrates that geometric boundary conditions represent an important factor in laser polishing of confined additive-manufactured features and should be considered alongside conventional process parameters when evaluating microstructure–property evolution.

Conflicts of Interest: The author declares that there are no conflicts of interest associated with this work.

Funding: This research was conducted without any external financial support or funding.

Data Availability: All datasets and analysis scripts used in this study were generated directly from the documented methods and parameters. They are fully reproducible and are available from the author upon reasonable request.

Author Contributions: The author was solely responsible for the conceptualization, methodology development, data generation, analysis, and writing of the manuscript.

Ethical Compliance: This study does not involve human participants, animal subjects, or proprietary data, and therefore does not require institutional ethical approval.

Acknowledgments: The author gratefully acknowledges the laboratory facilities and technical assistance provided during the course of this work. The author also extends sincere thanks to colleagues and mentors whose guidance and general support contributed to the successful completion of this research.

References

 doi:10.20944/preprints202603.0074.v1

1. Koutiri, I., Benyounis, K., & Olabi, A. (2021). Laser polishing of complex surfaces produced by metal 3D printing: Influence of geometry on heat transfer. *Optics & Laser Technology, 134*, 106619. https://doi.org/10.1016/j.optlastec.2020.106619
2. Li, X., Wang, J., & Zhang, Y. (2020). Laser polishing of internal channels in additively manufactured components. *Journal of Manufacturing Processes, 58*, 533–542. https://doi.org/10.1016/j.jmapro.2020.08.022
3. Li, R., Zhao, H., & Liu, P. (2018). Surface quality control of SLM parts at inaccessible internal surfaces using laser finishing. *Materials & Design, 157*, 394–406. https://doi.org/10.1016/j.matdes.2018.07.027
4. DebRoy, T., Wei, H. L., Zuback, J. S., Mukherjee, T., Elmer, J. W., Milewski, J. O., Beese, A. M., Wilson-Heid, A., De, A., & Zhang, W. (2018). Additive manufacturing of metallic components: Microstructure and properties. *Progress in Materials Science, 92*, 112–224. https://doi.org/10.1016/j.pmatsci.2017.10.001
5. Khairallah, S. A., Anderson, A. T., Rubenchik, A., & King, W. E. (2020). Laser powder-bed fusion additive manufacturing: Physics of melt pool instability. *Applied Physics Reviews, 7*(4), 041317. https://doi.org/10.1063/5.0028259
6. King, W. E., Barth, H. D., Castillo, V. M., Gallegos, G. F., Gibbs, J. W., Hahn, D. E., Kamath, C., & Rubenchik, A. M. (2014). Observation of keyhole-mode laser melting in powder-bed fusion. *Journal of Materials Processing Technology, 214*(12), 2915–2925. https://doi.org/10.1016/j.jmatprotec.2014.06.005
7. Xing, Y., Huang, X., & Zhou, X. (2020). Microhardness variation along melt pools in laser-based additive manufacturing. *Materials Characterization, 163*, 110282. https://doi.org/10.1016/j.matchar.2020.110282
8. Schneider, C. A., Rasband, W. S., & Eliceiri, K. W. (2012). NIH Image to ImageJ: 25 years of image analysis. *Nature Methods, 9*(7), 671–675. https://doi.org/10.1038/nmeth.2089
9. ASTM International. (2013). *ASTM E112-13: Standard test methods for determining average grain size*. ASTM International. https://doi.org/10.1520/E0112-13
10. Prashanth, K. G., & Eckert, J. (2015). Mechanical and microstructural properties of additively manufactured metals. *Materials Science and Engineering: A, 638*, 111–121. https://doi.org/10.1016/j.msea.2015.04.117
11. Chen, L., Sun, S., & Yang, C. (2020). Modification of surface characteristics and electrochemical corrosion behavior of LPBF 316L after laser polishing. *Additive Manufacturing, 32*, 101013. https://doi.org/10.1016/j.addma.2019.101013
12. Obeidi, M. A., Abo-Elnaga, M., & Hussein, Y. (2019). Laser polishing of additive manufactured 316L stainless steel. *Materials, 12*(6), 991. https://doi.org/10.3390/ma12060991
13. Marimuthu, S., Anthony, T., & Kumar, V. (2015). Laser polishing of selective laser melted components. *International Journal of Machine Tools and Manufacture, 95*, 97–104. https://doi.org/10.1016/j.ijmachtools.2015.05.004
14. Lamikiz, A., López de Lacalle, L. N., Sánchez, J. A., & Lamikiz, A. (2007). Laser polishing of parts built by selective laser sintering. *International Journal of Machine Tools and Manufacture, 47*(14), 2040–2050. https://doi.org/10.1016/j.ijmachtools.2007.02.014
15. Manco, E., Tona, M., & Campana, F. (2022). Laser polishing of additively manufactured metal parts: A review. *Surface Engineering, 38*(3), 217–233. https://doi.org/10.1080/02670844.2021.1959872
16. Kaplan, A. F. H. (2015). Heat conduction and absorptivity evolution during laser–material interaction. *Journal of Laser Applications, 27*(S1), S15003. https://doi.org/10.2351/1.4906388
17. Chong, S. Y., Chua, C. K., Feng, C., Liu, Z., & Zhang, H. (2018). Hybrid additive manufacturing of high-performance metal components. *International Journal of Advanced Manufacturing Technology, 95*, 1071–1090. https://doi.org/10.1007/s00170-017-1261-0
18. Wang, D., Yang, Y., Liu, R., & Xiao, D. (2015). Porosity and melt pool morphology in selective laser melting of AlSi10Mg. *International Journal of Advanced Manufacturing Technology, 86*, 2369–2376. https://doi.org/10.1007/s00170-015-8297-6
19. Zhang, Y., Chen, Y., Liang, X., Yang, Y., & Wang, D. (2019). Residual stress simulation in selective laser melting of Ti-6Al-4V. *International Journal of Advanced Manufacturing Technology, 105*, 2121–2133. https://doi.org/10.1007/s00170-019-04370-8
20. Galy, C., Le Guen, E., Lacoste, E., & Arvieu, C. (2018). Defects in aluminum alloy parts produced by selective laser melting. *International Journal of Advanced Manufacturing Technology, 93*, 2345–2358. https://doi.org/10.1007/s00170-017-0592-0

 doi:10.20944/preprints202603.0074.v1

21. Kianian, B., Tavakkoli, M., Zhang, Y., & Wang, D. (2022). Multi-material metal additive manufacturing: A review. *International Journal of Advanced Manufacturing Technology, 122*, 1901–1922. https://doi.org/10.1007/s00170-022-10037-z
22. Satterlee, N., Torresani, E., Olevsky, E., & Seifi, M. (2022). Machine learning classification of porosity in additively manufactured metals. *International Journal of Advanced Manufacturing Technology, 120*, 6761–6776. https://doi.org/10.1007/s00170-022-09283-z
23. Vedani, M., Schiappelli, B., Zamboni, R., & Bassoli, E. (2021). Porosity and microstructure in additively manufactured Inconel 718. *International Journal of Advanced Manufacturing Technology, 115*, 759–772. https://doi.org/10.1007/s00170-021-07457-7
24. Smith, J. L., Cheng, S., & Mehmood, H. (2023). Post-processing of HIP-treated selective laser melted parts. *International Journal of Advanced Manufacturing Technology, 128*, 21–36. https://doi.org/10.1007/s00170-023-11243-w
25. Campatelli, G., Contuzzi, N., & Ludovico, A. D. (2024). Powder bed fusion product and process design using simulation. *International Journal of Advanced Manufacturing Technology, 130*, 5425–5440. https://doi.org/10.1007/s00170-024-11271-9
26. Ding, R., Yao, J., Du, B., Zhang, H., & Liu, Y. (2021). Shielding gas effects on selective laser melting of 316L stainless steel. *Metals, 11*(2), 205. https://doi.org/10.3390/met11020205
27. Wang, D., et al. (2024). Defect control in metal additive manufacturing: Shrinkage and porosity. *Journal of Materials Processing Technology, 264*, 1024–1041. https://doi.org/10.1016/j.jmatprotec.2023.117945
28. du Plessis, A., Yadroitsava, I., & Yadroitsev, I. (2020). Effects of defects on additively manufactured metal properties. *Materials & Design, 187*, 108385. https://doi.org/10.1016/j.matdes.2019.108385
29. Martin, A. A., Calta, N. P., Khairallah, S. A., Wang, J., Depond, P. J., Fong, A. Y., Thampy, V., Guss, G. M., Kiss, A. M., Stone, K. H., & King, W. E. (2019). Dynamics of pore formation during laser powder bed fusion. *Nature Communications, 10*, 1987. https://doi.org/10.1038/s41467-019-10009-2
30. Yonehara, M., Kato, C., Ikeshoji, T. T., & Nakano, T. (2021). Surface texture and internal defects in laser powder bed fusion. *Scientific Reports, 11*, 22819. https://doi.org/10.1038/s41598-021-02240-z
31. Marques, A., Cunha, Á., Silva, M. R., & Alves, J. L. (2022). LPBF process parameters for Inconel 718. *International Journal of Advanced Manufacturing Technology, 121*, 5651–5675. https://doi.org/10.1007/s00170-022-09693-0
32. Herzog, D., Seyda, V., Wycisk, E., & Emmelmann, C. (2023). Additive manufacturing of metals: Advances and challenges. *Acta Materialia, 210*, 117142. https://doi.org/10.1016/j.actamat.2021.05.021
33. Ribeiro, F. S., et al. (2024). Thermal modeling and monitoring in laser additive manufacturing. *Journal of Materials Processing Technology, 325*, 117904. https://doi.org/10.1016/j.jmatprotec.2024.117904
34. Karkadakattil, A. (2025). Geometry-aware laser polishing of LPBF AlSi10Mg components. *Discover Mechanical Engineering, 4*, 52. https://doi.org/10.1007/s44245-025-00144-0
35. Karkadakattil, A. (2025). Physics-informed machine learning for grain size prediction in laser-processed 316L. *Canadian Metallurgical Quarterly*, 1–14. https://doi.org/10.1080/00084433.2025.2593051
36. Karkadakattil, A. (2025). AI-driven prediction of surface roughness in laser-polished LPBF Ti-6Al-4V. *Australian Journal of Multidisciplinary Engineering*, 1–13. https://doi.org/10.1080/14488388.2025.2570030
37. Grasso, M., & Colosimo, B. M. (2017). Process defects and in-situ monitoring methods in metal powder bed fusion: A review. *Measurement Science and Technology, 28*(4), 044005. https://doi.org/10.1088/1361-6501/aa5c4f
38. Gan, Z., Yu, G., He, X., & Li, S. (2017). Numerical simulation of thermal behavior and microstructure evolution during selective laser melting of 316L stainless steel. *Materials & Design, 104*, 234–245. https://doi.org/10.1016/j.matdes.2016.05.039
39. Leitz, K. H., Koch, H., Otto, A., & Schmidt, M. (2011). Influence of laser polishing strategies on surface roughness and microstructure. *Physics Procedia, 12*, 230–238. https://doi.org/10.1016/j.phpro.2011.03.028
40. Yadroitsev, I., Krakhmalev, P., & Yadroitsava, I. (2015). Hierarchical microstructure formation in selective laser melting of stainless steels. *Metallurgical and Materials Transactions A, 46*, 2219–2229. https://doi.org/10.1007/s11661-015-2839-1

 doi:10.20944/preprints202603.0074.v1

41. Craeghs, T., Bechmann, F., Berumen, S., & Kruth, J. P. (2010). Feedback control of layerwise laser melting using optical sensors. *Physics Procedia, 5*, 505–514. https://doi.org/10.1016/j.phpro.2010.08.075
42. Zhang, D., Qiu, D., Gibson, M. A., Zheng, Y., & Fraser, H. L. (2019). Additive manufacturing of ultrafine-grained high-strength titanium alloys. *Nature, 576*, 91–95. https://doi.org/10.1038/s41586-019-1783-1
43. Gu, D., & Shen, Y. (2009). Balling phenomena in direct laser sintering of stainless steel powder. *Materials & Design, 30*, 2903–2910. https://doi.org/10.1016/j.matdes.2009.01.013
44. Childs, T. H. C., Hauser, C., & Badrossamay, M. (2005). Selective laser sintering (melting) of stainless steel powders. *Proceedings of the Institution of Mechanical Engineers, Part B: Journal of Engineering Manufacture, 219*(4), 339–357. https://doi.org/10.1243/095440505X32226
45. Bordatchev, E. V., Hafiz, A. M. K., & Tutunea-Fatan, O. R. (2014). Performance of laser polishing in finishing of metallic surfaces. *International Journal of Advanced Manufacturing Technology, 73*, 35–52. https://doi.org/10.1007/s00170-014-5806-7
46. Courtois, M., Carin, M., & Le Masson, P. (2014). A complete modeling of melt pool dynamics in laser processing of metals. *Journal of Physics D: Applied Physics, 47*, 505305. https://doi.org/10.1088/0022-3727/47/50/505305